SRTTU

JCARME

ISSN: 2228-7922

Journal of Computational and Applied Research in Mechanical Engineering
Vol. 6, No. 2, pp. 115-127
http://jcarme.srttu.edu

Enhancing the low cycle fatigue strength of AA6061 aluminum alloy by using the optimized combination of ECAP and precipitation hardening

M. Jooybari [a], J. Shahbazi Karami [b] and M. Sheikhi [b,*]

[a] School of Mechanical Engineering, College of Engineering, University of Tehran, Tehran, Iran
[b] Faculty of Mechanical Engineering, Shahid Rajaee Teacher Training University, Tehran, Iran

Article info:

Received: 17/01/2016
Accepted: 18/12/2016
Online: 03/03/2017

Keywords:
Low cycle fatigue,
Equal channel angular Al alloy,
Ultra-fine grained microstructure,
Precipitation hardening.

Abstract

In the present study, mechanical properties and low cycle fatigue behavior of a solid-solutionized AA6061 aluminum alloy produced by equal channel angular pressing (ECAP) process were investigated. The grain refinement after two passes of ECAP significantly increased the yield stress and ultimate tensile stress and decreased the ductility of the alloy. However, the improvement of low cycle fatigue strength was not as remarkable as expected. Post-ECAP aging heat treatment to the peak-aging condition imposed a notable change in the strength and ductility of the alloy so that its fatigue strength partly enhanced. An optimized combination of grain refinement and distributed fine precipitates in the matrix of the alloy was achieved by conducting aging heat treatment between passes of ECAP. The proposed procedure was proved to yield the best combination of strength and ductility, better distribution and size of precipitates, and thus a remarkable improvement in the low cycle fatigue response of the investigated material.

Nomenclature

W: CG material in unstable solution treated temper

E2: UFG material underwent 2 passes of ECAP

$E2A_{Peak}$: UFG material after 2 passes of ECAP, aging heat treated for 210 minutes to the peak-aging condition

$E2_{Opt}$: UFG material aging treated after each pass of ECAP (in total 2 passes of ECAP and 210 minutes heat treatment)

Φ: Intersection angle of channels of the ECAP die

Ψ: curvature angle of the outer point of intersection of ECAP die

*Corresponding author
email address: m.sheikhi@srttu.edu

1. Introduction

Aluminum alloys are the most attractive non-ferrous materials playing an important role in engineering, especially in aerospace engineering. They have good corrosion resistance, as well as superior mechanical properties and light weight [1, 2]. During the last century, alloying and age hardening capabilities of Al alloys in improving their strength were discovered. However, recently it has been realized that the grain refining processes improves the mechanical and functional properties of these alloys [3-5]. During last years, using SPD processes in producing ultra-fine grain (UFG) materials have become attractive to researchers because of their striking effects on mechanical properties of materials. During a Severe Plastic deformation (SPD) process, a very high level of strain is applied to the material [6-14]. There are different types of SPD processes such as accumulative roll-bonding (ARB), high- pressure torsion (HPT), and equal channel angular pressing (ECAP). Among these processes, ECAP seems to be the most attractive, and potentially the most useful process [15].

A work piece with a rectangular or circular cross-section is pressed through a die during the ECAP process. The die contains two equal cross-section channels which intersect at an angle of φ. There is another angle Ψ, which defines the arc of curvature at the outer point of intersection of the two channels. The geometry of the ECAP die is shown in Fig. 1. As the material crosses the intersection between channels it is mainly deformed by a shear mechanism combined with a high hydrostatic pressure as a consequence of the constraint imposed by the die. The introduced severe plastic deformation in the material causes a reduction in grain size and therefore the mechanical properties of the material improve dramatically [16-18].

The advent of SPD processes make a dramatic contribution to the improvement of fatigue behavior of Al alloys. The fatigue behavior of nanostructured and UFG Al alloys produced by sever plastic deformation have been studied by numerous researchers [3, 19-25].

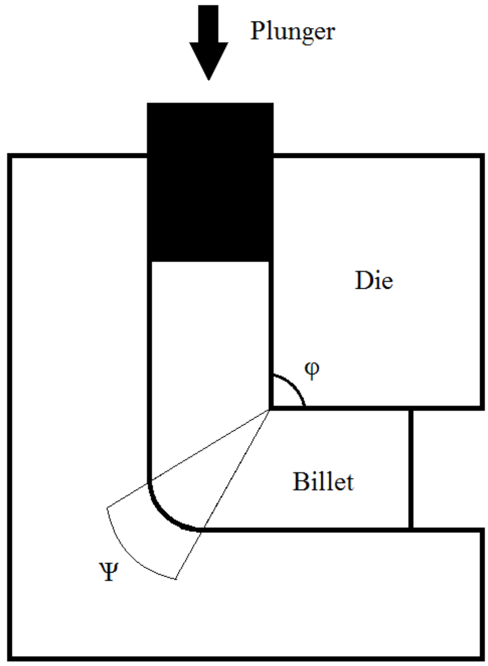

Fig. 1. Schematic of the ECAP process.

Some of these reports are contradictory. For example, a large enhancement in fatigue life of AA6061 alloy by ten times in high cycle frequency (HCF) regime was reported after a single ECAP pass. However, by increasing the ECAP passes to four, this effect disappeared due to a significant increase in the fraction of high angle grain boundaries [21]. The AA2124 alloy showed a higher fatigue life after eight ECAP passes compared with the four-pass ECAPed alloy and complex microstructure was observed in both conditions [24].

It is found that unlike the significant effect of SPD processes in enhancing the tensile strength of Al alloys, sometimes the resulted grain refinement does not have a notable influence on fatigue behavior of these alloys in high cycle regime compared to its effect on tensile properties. On the other hand, because of the negative effect of grain refinement on the ductility of Al alloys on monotonic and cyclic deformation which promotes early crack initiation and a higher fraction of grain boundaries favorable for crack propagation, the

low cycle fatigue (LCF) of these alloys is of high complexity [20]. As a consequence, some researchers investigated different measures to improve the HCF and LCF behavior of Al alloys. Vinogradov et al. argued that the loss of ductility during severe hardening through ECAP is the main reason for the low LCF life of UFG materials. They also claimed that another factor which is responsible for the fatigue life of UFG materials is their susceptibility to strain localization as a result of increasing strain hardening and decreasing ductility. Therefore, finding a suitable combination of affecting factors such as strength and ductility is necessary to achieve a desirable fatigue behavior [26, 27].
Kim et al. introduced the combination of Pre–ECAP solution treatment and post–ECAP aging treatment as an effective method to enhance the strength and superplasticity of an AA6061 alloy. By implementing six passes of ECAP and post-ECAP aging, the largest increase in ultimate tensile strength (UTS) and yield stress (YS) of the alloy was obtained. What is more, the results of the research were striking in comparison with pre–ECAP peak-aging treatment studied by other investigators [28].
Höppel et al. [29] in an investigation on the optimization of the fatigue behavior of UFG Al alloys produced by ECAP, and by considering the results of other researchers [27, 30-34], reported that the investigated UFG Al alloys exhibited shorter fatigue lives in an LCF regime than Coarse grained (CG) counterparts. They proposed that the fatigue lives could be enhanced appreciably by a suitable heat treatment following ECAP because of an increase in the ductility.
Malekjani et al. have investigated the cyclic response of UFG AA2024 alloy produced by cryo-rolling and the effect of precipitates on the cyclic stability. Grain refining reduced the fatigue life of the alloy under strain controlled fatigue test. Moreover, the fatigue performance of the peak-aged samples was higher than the under aged samples because of their higher fatigue ductility coefficient and higher cyclic hardening. On the other hand, at lower strain amplitudes the fatigue life of the peak-aged samples tended to decrease, which might be due to a much lower contribution of plastic strain amplitude against the elastic strain amplitude in that range [19].
In a study on the strain-controlled fatigue behavior of AA6060 alloy, a combination of ECAP and aging treatment was investigated. Three series of samples were prepared; two of them were at peak- age condition (T6) before pressing, and then subjected to two and eight passes of ECAP. A ductility-optimized condition was achieved for the third sample by a solution heat treatment before two passes of ECAP followed by a short aging treatment. The results demonstrated that the optimized condition leads to a slight cyclic hardening at the very first few cycles followed by a linear softening meaning that the thermally induced recovery does not prevent cyclic softening in the ongoing fatigue process. Moreover, although the optimized specimen shows a higher ductility and strain hardening capability in monotonic loading than its as-processed counterpart E2, its performance in strain-controlled fatigue life remains below the expectations; maybe because of the formation of extraordinarily fine precipitates after ECAP, which make the optimized condition more prone to shear localization in deformation bands [35].
X-Ray studies of Sitdikov et al. on dynamic aging in AA6201 alloy produced by SPD process determined the quantitative characteristics of the size, shape and spatial distribution of the secondary phase particles formed in the alloy during dynamic aging. Their results were solid in making difference between the inherent characteristics of dynamic strain aging and conventional T6 treatment regarding their microstructural data. These findings would definitely be promising in future studies on fatigue behavior of the alloys strengthened by such methods [36].
The present study focuses on LCF behavior of AA6061 alloy produced by ECAP combined with aging heat treatment to achieve a suitable LCF properties by finding the appropriate combination of ECAP and precipitation hardening. To the authors' best knowledge there is no record in the literature which investigates the effect of performing aging heat treatment between the passes of SPD process on the fatigue behavior of Al alloys. Since the size, density, and

distribution of secondary phases are important in strengthening the alloy, and also because the balance in ductility and tensile strength of the alloy, which can be influenced by post/pre ECAP aging treatments, is determinative of fatigue crack propagation as a controlling factor of the LCF response [22, 23, 37], one can predict that implementing such a combined procedure would be influencing.

2. Material and experimental procedures

2.1. Material, conditions, and ECAP processing

In this investigation, a precipitation hardened Al-Mg-Si aluminum alloy, designated as AA6061, in the form of 20 mm diameter and 100 mm length rods was used. The chemical composition of the alloy is shown in Table 1. Billets of the alloy were first annealed to remove dislocations and to restore the original workability of the alloy. The annealing procedure was performed at 413 °C for 2.5 h by post cooling at room temperature. The samples were then solution heat treated at 527 °C for 90 min followed by rapid quenching in cold water. The aim of this heat treatment was to produce a super-saturated condition for the alloy and to prepare the samples for aging procedures.

Table 1. Chemical composition of the AA6061 alloy used for experiments.

Si	Fe	Cu	Mn	Mg	Cr	Ni	Zn	Ti	Be	Ca	Li
0.73	0.11	0.32	0.008	1.30	0.16	0.01	0.07	Trace	Trace	Trace	Trace
Pb	**Sn**	**Sr**	**V**	**Na**	**Bi**	**Co**	**Zr**	**B**	**Ga**	**Cd**	**Al**
Trace	<0.005	Trace	0.006	Trace	<0.004	<0.002	Trace	<0.001	Trace	Trace	Base

ECAP was performed using a die-set with an intersection angle of 90 ° by route B (90° rotation of sample along its axis, this route yields the most homogeneous microstructure with the finest grains and high angle grain boundaries [38]) at room temperature by a hydraulic press with a ram speed of 1 mm/min. For more details of the ECAP-process refer to [4, 38].

Aging procedure was performed on the samples at 160 °C for different periods of time. To find the time required for the peak-age condition, eight disks were cut from the one pass ECAPed specimen and aged for 0 to 690 min (with the time increment of 70 min). The micro-Vickers hardness was measured on the cross-sectional plane, perpendicular to the pressing direction of the ECAPed specimens. The microhardness measurements were performed with a load of 100 g for a dwell time of 30 s at 3 different points around the center of the samples and the average values were reported. Based on these results, the AA6061 material was processed in three different conditions. For the first group of specimens, 2 passes of ECAP were performed on the as-quenched material. For the second condition, samples were subjected to two passes of ECAP followed by aging heat treatment for 210 min to the peak-aged condition. The third series of samples were produced by two passes of ECAP, and after each pass of pressing, aging treatment was conducted for 105 min (half of the time needed for peak-aging condition). The details of the procedures performed on the specimens are given in Table 2.

Table 2. Different conditions of the samples, their designation and procedures for preparation.

Name	Procedure
W	Solution treated, As-quenched, without any deformation or further heat treatment*
E2	Solution treated, subjected to two passes of ECAP*
E2-A_{Peak}	Solution treated, two passes of ECAP, then aged at 160 °C for 210 min to the peak-aging condition
E1AE1A ($E2_{Opt}$)	Solution treated, one pass of ECAP, aged at 160 °C for 105 min, one another pass of ECAP, again aged for 105 min (i.e. the time required for peak-aging condition is divided between ECAP passes)

* Samples were kept in the refrigerator in order to avoid unwanted precipitations

2.2. Materials testing

Monotonic axial tensile tests were conducted at the strain rate of 0.1 mm/min, using round samples with a diameter of 4 mm and a gauge length of 20 mm extracted from the central parts of the ECAPed rods according to ASTM E 8m-04.

Round Dog-bone fatigue test specimens were machined from the center of the ECAPed samples according to ASTM E466-96 with the gauge diameter of 6 mm, gauge length of 24 mm, and curve arc equal to 48 mm. All samples were well surface finished and then subjected to cyclic axial loading under stress control using a stress ratio of R = -1 (i.e. symmetric push-pull), and at the frequency of 30 Hertz on Instron 8502 machine. Fatigue tests were conducted on samples at different stress amplitudes equal to 0.9 UTS, 0.8 UTS, 0.7 UTS of each sample. Moreover, in order to well compare the fatigue behavior of the processed samples (E2, $E2A_{Peak}$, and $E2_{Opt}$), fatigue loading was also carried out at single stress amplitude 0.6 times the average of the ultimate tensile strength values of these three samples.

2.3. Microstructural investigations

Microstructural investigations were performed by optical microscopy (OM) with normal and polarized light, and scanning electron microscopy (SEM) on UFG specimens to observe the microstructural development, precipitates size and distribution, and the fracture surface of fatigued samples.

3. Results and discussion

3.1. Microstructures of processed materials

Optical microscopy with normal and polarized lights on samples provided different images of microstructures prior to fatigue loading (Figs. 2-7). Microstructural characteristics relevant to the fatigue behavior are discussed below.

3.1.1. E2 condition

In this condition, the material was subjected to two passes of ECAP without subsequent aging treatment. However, some small and erratically dispersed precipitates can be seen in the microstructure as a result of unwanted subtle natural aging (Fig. 2). In addition, Fig. 3 shows that the grains are elongated and stretched out in the direction of shear and a small but significant fraction of grain boundaries revealed a high-angle misorientation.

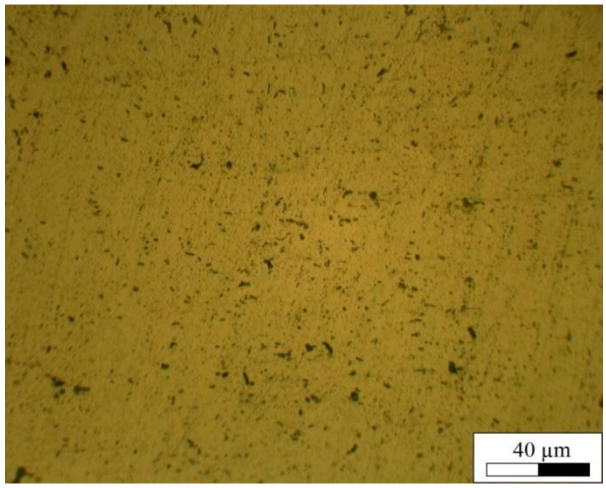

Fig. 2. Unwanted precipitates which are very fine and scares; specimen E2 (without aging).

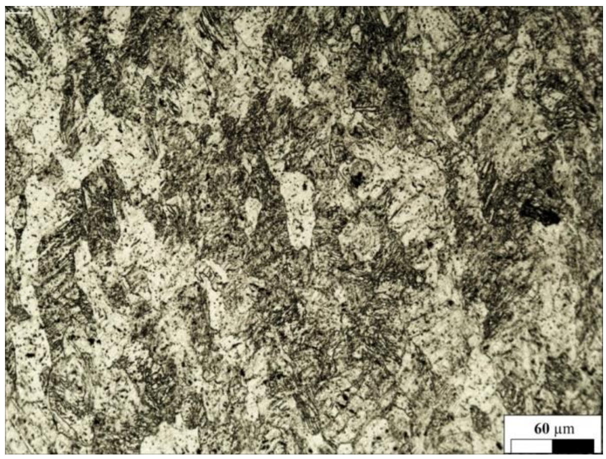

Fig. 3. Very fine and elongated grains resulted from ECAP; specimen E2.

3.1.2. $E2A_{Peak}$ condition

By conducting 210 min aging heat treatment on the material in E2 condition and developing it to a peak-aged material, the $E2A_{Peak}$ condition was obtained. As Fig. 4 demonstrates, after the heat treatment, precipitate particles apparently increased in both volume fraction and size. Some larger precipitates are also presented in the matrix which may contain impurities and may lead to the formation of precipitate-free zones. The observed microstructure by polarized light microscopy well defines the effects of recovery and recrystallization due to the heat treatment on grain size and boundaries as the elongated grains and HAGBs are less frequent in this condition. Again, large precipitates inherent in peak-aged condition are obvious in Fig. 5 comparing with Fig. 3.

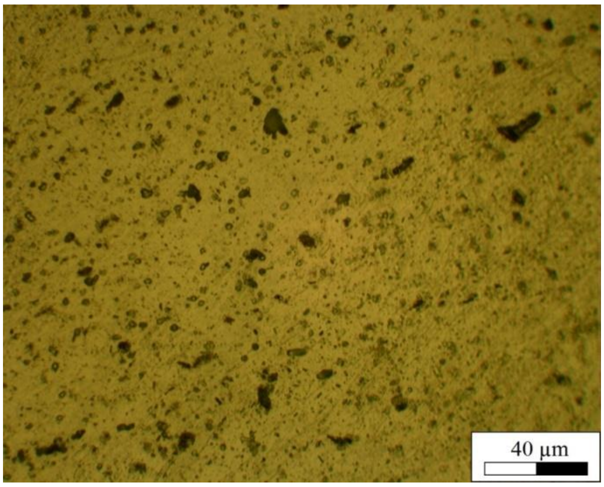

Fig. 4. Large and abundant precipitates in peak-aged UFG specimen, $E2A_{Peak}$.

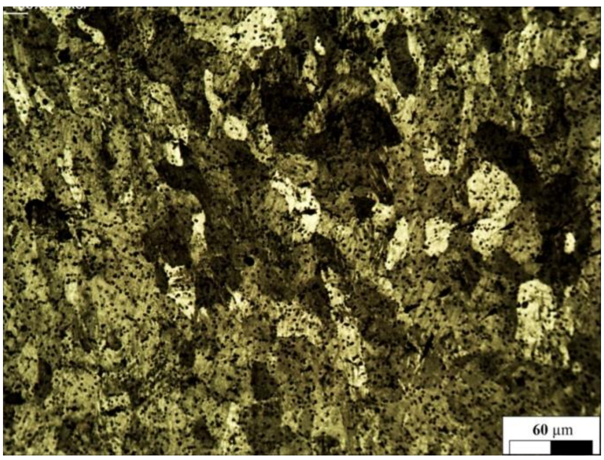

Fig. 5. Large precipitates along with recovered crystals as a result of peak aging, specimen $E2A_{Peak}$.

3.1.3. $E2_{Opt}$ condition

The material reached to the peak-aging (or near peak-aging) condition but in a two-stage sequence of ECAP and aging heat treatment. After the first pass of ECAP, some level of grain refinement is achieved and the structure contains a high fraction of non-equilibrium grain boundaries. In this condition, the alloy has a high strength with a subtle decrease in ductility. By the first period of aging treatment very fine precipitate particles with strengthening effect appear in the microstructure. On the other hand, this thermal activation facilitates the recovery process and it leads to a reduction in the fraction of HAGBs which has a softening effect as well as inducing some level of increase in ductility of the alloy. The result is a condition with reasonable strength and acceptable ductility. The second pass of ECAP induces microstructural distortion in the material and again a large number of HAGBs appears. Moreover, the very fine precipitates of the first stage of aging completely spread in the distorted microstructure. By implementing the second phase of aging, the formation of precipitates starts rapidly due to the increased number of diffusion pathways. Now, a very fine size and good distribution of these precipitates are achieved because of numerous nucleation sites in the highly distorted microstructure. As a consequence, a condition is achieved which has a good combination of recovered but not recrystallized microstructure (because of eliminating the time of heat treatment by dividing it between passes of ECAP) and a high number of HAGBs and fine distribution of precipitates (Figs. 6 and 7). It means that the optimized sample supposedly has a higher strength and ductility compared to the other ECAPed samples. Since the balance of these two tensile characteristics is vital in LCF behavior, one may conclude that the $E2A_{Opt}$ most likely has the best fatigue response in low cycle regime.

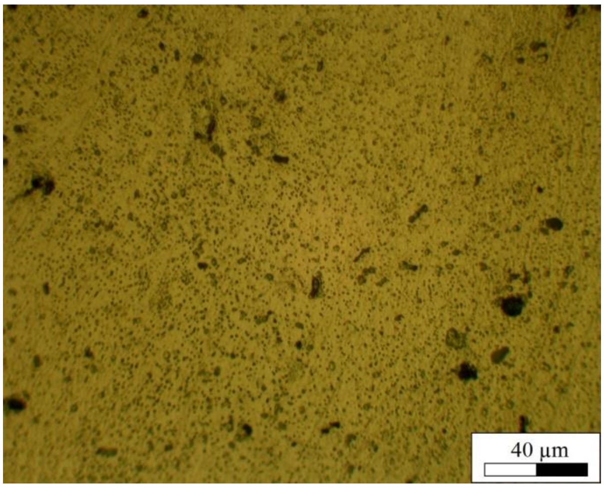

Fig. 6. Small size particles with high density and distribution in the matrix of alloy in $E2_{Opt}$ condition.

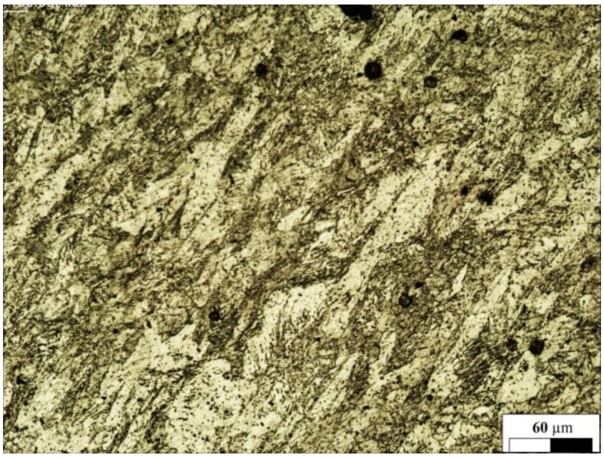

Fig. 7. Very distorted microstructure with large number of completely dispersed precipitates, $E2A_{Opt}$ condition.

3.2. Stress-strain response

Results of tensile tests on different samples are shown in Fig. 8, and Table 3. Notable differences between the CG and three UFG conditions can be observed. These data shows that the optimized combination of grain refinement and precipitation hardening yields the highest ultimate tensile strength. However, its total elongation to failure as a criterion of ductility is not the best among three UFG conditions. The maximum value of total elongation belongs to the peak-aged condition (i.e. $E2A_{Peak}$) but its difference from that of $E2_{Opt}$ is not significant (0.62%). Thus it can be concluded that the chosen strategy is optimized regarding the tensile properties.

In addition to the balance of tensile strength and ductility, another factor is involved in the LCF behavior of metallic materials. The ratio of UTS/YS as a measure of strain hardening capability is used to estimate the cyclic softening or hardening of the alloy during fatigue loading. According to Manson and Hirschberg [39], if the ratio of UTS/YS is more than 1.4, the material undergoes the cyclic hardening. For the ratios lower than 1.2, material softens with increasing the number of cycles. Materials with a ratio of UTS/YS between 1.2 and 1.4 are somehow stable in cyclic loading and the stress amplitude does not significantly increase or decrease during cyclic loading. Among the UFG alloys of the present study, this ratio is higher than 1.4 for the optimized $E2_{Opt}$ condition which shows its probable hardening trend in cyclic loading. One can predict that the samples produced by this optimized procedure would show a rapid decrease in the slope of S-N curve after a few cycles.

Table 3. Tensile properties of different investigated samples.

Sample	UTS (MPa)	YS, 0.2 % (MPa)	Total elongation (%)	UTS/YS
W	245	132	27.18	1.856
E2	412	327	10.68	1.26
$E2A_{Peak}$	398	297	15.59	1.34
E_{Opt}	421	281	14.97	1.498

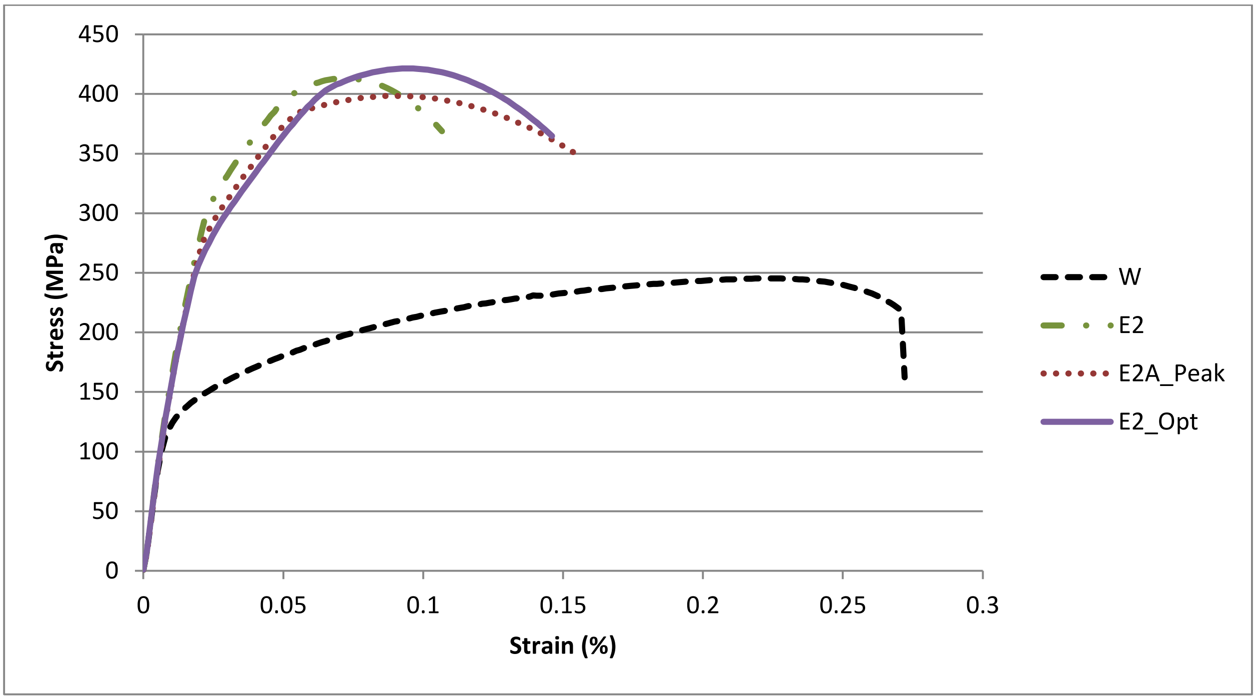

Fig. 8. Stress-strain curves obtained by conducting tensile tests on the specimens.

3.3. Stress controlled fatigue test

Results of the fatigue tests in low cycle regime are shown in Fig. 9 as Wöhler S–N curves for different samples of the present study with additional data of AA6061-T6 extracted from [42].

The curves show that grain refinement has a significant effect on the S-N fatigue response of AA6061 alloy. It can be related to the higher tensile strength of UFG material. However, increasing the number of cycles leads to an abrupt and remarkable decrease in fatigue strength. Post-ECAP aging heat treatment generally has a positive effect on the LCF life of the alloy and suppresses the negative effect of grain refinement at higher numbers of cycles as a result of the strong function of the increased ductility. In addition, the samples do not show such an accelerated softening at the onset of cyclic straining, as recovery processes were already activated during aging. Similar results were observed in [29] and [31] as the post-ECAP treatments was shown to be effective to limit cyclic softening. Furthermore, in another reference [40] where a particular aging treatment led to a post-ECAP peak-age condition with an excellent combination of strength and ductility, similar trend was indicated. This is likely because of the stabilizing effects of post-ECAP heat treatment on the UFG microstructure.

Among the UFG samples, the optimized condition ($E2_{Opt}$) provides the best LCF response as at the same stress amplitude of 246 MPa its fatigue failure happens at an approximately 101900 cycles compared to 46600 and 18800 cycles to failure respectively for $E2A_{Peak}$ and E2 conditions. This significant better function of the optimized condition than the peak-aged, despite its lower ductility, is because of the great influence of cyclic hardening capability of this particular condition as its ratio of UTS/YS indicates. However, this ratio is not a reliable factor in determining the fatigue behavior of UFG material, because the nature of fatigue consists of numerous complex mechanisms such as grain size, precipitate content, size and spatial distribution, stacking fault energy and the attendant equilibrium spacing of partial dislocations, and crystallographic texture [41].

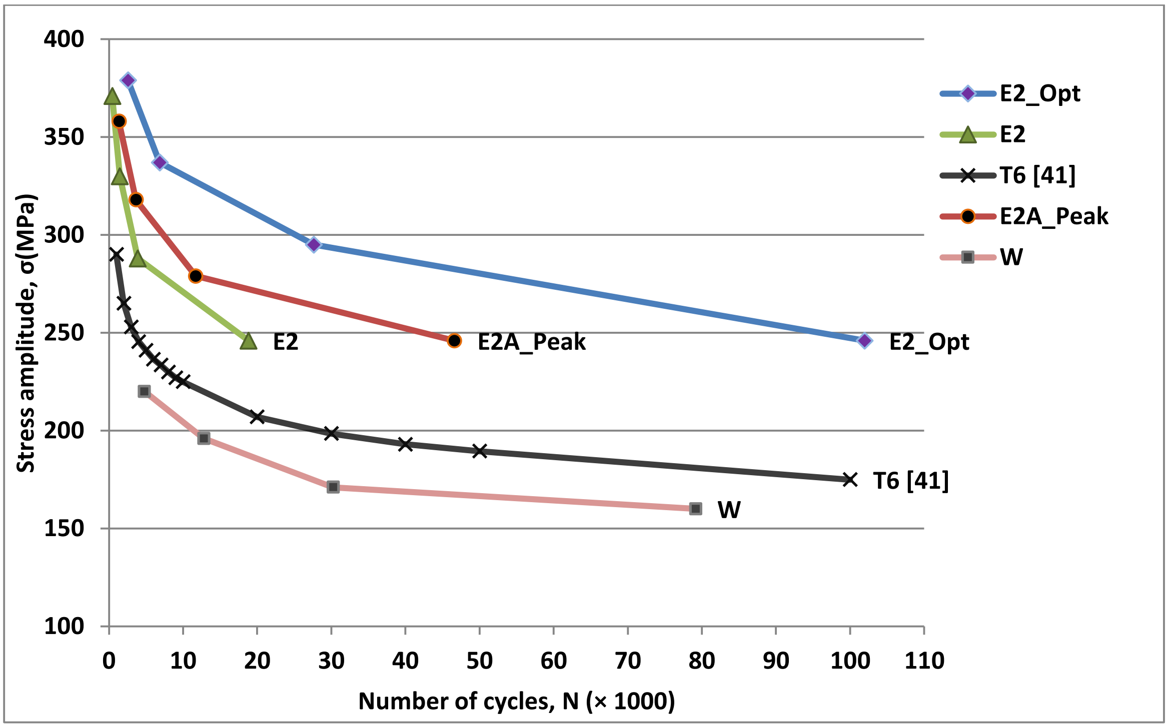

Fig. 9. S-N curves for the studied specimens; data of T6 extracted from [42] is embedded here for comparison purposes.

Generally, the grain refinement enhances the resistance to fatigue crack initiation by decreasing the number of dislocations in slip bands. This reduces the depth of surface fatigue markings and by increasing the yield stress which restricts the macroscopic plastic deformation in the beginning of cyclic loading. On the other hand, the resistance to crack growth decreases with the grain refinement. In the near-threshold of fatigue crack growth, UFG materials exhibit a faster rate of crack propagation because of the reduced level of fracture surface roughness seen in the finer grained metal, as the deflections in crack path promoted during crystallographic crack advance are reduced with grain refinement [43]. LCF behavior is mainly controlled by fatigue crack propagation. In addition, the formation of necking zone occurs in this regime; therefore, the fatigue fracture mostly takes place by joining of microvoids in the microstructure of the alloy [22, 23, 37]. It can be concluded that ductility play a key role in fatigue response at higher stress amplitude.

Furthermore, aging heat treatment induces precipitates effective in changing the microstructural nature of the material. The performance of the precipitates under cyclic loading conditions may vary, depending on their size and structural characteristics. When dislocations cut through precipitates, a local decrease to further dislocation motion and consequently concentration of slip taken place [44, 45]. Apart from the role of big constituent particles in crack initiation, concentration of slip caused by the easy path of dislocations movement will normally ease the crack initiation stage. On the other hand, when the particle is not cut, dislocations form loops at the interfaces resulting in more homogenous deformation, which prevents strain localization and crack initiation [46, 47]. Moreover, difference in the cyclic hardening behavior of peak-aged and optimized aging conditions might be related to the state of precipitates in terms of their size and coherency with the matrix. It was shown earlier that precipitates in the optimized condition ($E2_{Opt}$) are smaller in size and have more coherent distribution which leads to the promoted stability of microstructure under cyclic loading and prevents grain boundary movement and grain coarsening [29].

3.4. Fracture surface analysis

SEM observations of the fractured surfaces of the alloy in E2A$_{Peak}$ and E2$_{Opt}$ conditions fatigued at the stress amplitudes of respectively 318 and 337 MPa are shown in Fig. 10. The SEM images show that the fractured surfaces have irregular conditions showing that the fatigue is resulted from different mechanisms of failure. The surfaces mostly consist of many microvoids and dimples (Fig. 10. B, C, D), indicating the ductile essence of fracture in the specimens. Dimples are slightly larger and deeper in the fracture surface of the E2$_{Opt}$ specimen (Fig. 10. D) comparing with the fracture surface of E2A$_{Peak}$ (Fig. 10. C). This may be an evidence of the better fatigue response of the alloy in this condition. In the fracture surface of E2A$_{Peak}$ specimen the presence of microvoids is more common which can be a reason for its lower fatigue strength than that of E2$_{Opt}$. When a microvoid is nucleated at a second phase particle, it propagates through the interface between the particle and surrounding matrix. Since the precipitates are inclined to be formed at high energy locations such as grain boundaries, the growing microvoid propagates through one grain boundary to the next and forms an intergranular fracture mode which is more common in E2A$_{Peak}$ as a result of large second phase particles (Fig. 10. B, D). On the other hand, in both specimens in some areas of the fractured surface, striations and brittle fracture are revealed despite the fact that at high stress amplitudes of fatigue loading, such a texture is not common. This is because the motion of dislocations does not have enough time to become large enough (Fig. 10. E, F). This phenomenon is more frequent in the optimized specimen (Fig. 10. F.), as it may fails at higher cycles compared to the peak-aged specimen.

4. Conclusions

Mechanical properties and low cycle fatigue behavior of a solid-solution treated AA6061 alloy produced by 2 passes of ECAP process were assessed through tensile and cyclic tests in terms of yield stress, ultimate tensile strength, total elongation and fatigue strength at different stress amplitudes. It was found that:

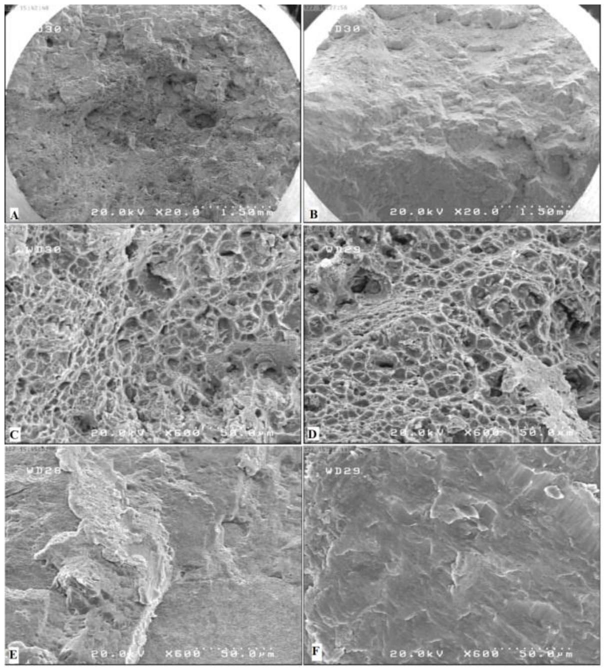

Fig. 10. Fatigue fractured surfaces of E2A$_{Peak}$ and E2$_{Opt}$ at the fatigue loading with the stress amplitude of respectively 318 and 337 MPa, and cycles to failure respectively 3640 and 6830. A: .

- Yield and ultimate tensile stresses of the 6061 Al alloy considerably increases after ECAP process, while ductility decreases.
- An enhancement occurs in fatigue strength of the material after 2 passes of ECAP. However, its fatigue strength tends to decrease by increasing the number of cycles which may be related to cyclic softening of the alloy.
- Aging heat treatment remarkably contributes to the balance of tensile properties and the increase in LCF response of the alloy. The effect of aging heat treatment would even be more significant if the time required for peak-aging is divided between passes of ECAP.
- The differences in fatigue behavior of aforementioned UFG specimens is attributed to the differences in grain boundary angle, size, density and distribution of second phase particles, and the ratio of UTS to YS as a cyclic hardening/softening criterion.
- OM observation of the cross-section of the samples clearly shows the transformation of crystals and second phase particles due to the

different procedures of severe plastic deformation and precipitation. Moreover, SEM analysis of the fractured surfaces of two of the fatigued samples gives a better understanding of the essence of the mechanisms causing fatigue failure. It is shown that the failure is not merely because of a single fatigue mechanism as different areas of dimples, microvoids, featureless cracks, and striations are seen, altogether showing that the border of ductile and brittle fracture is not clear. It can be attributed to the high level of stress in which these two samples are failed. Nevertheless, the fracture surfaces of these two samples have some differences, however, slight.

References

[1] G. E. Totten, C. E. Bates and G. M. Webster, "Physical Metallurgy and Processes", *Handbook of Aluminum*, Eds. G. E. Totten, and D. S. MacKenzie, Marcel Dekker Inc., New York, Vol. 1, (2003).

[2] I. J. Polmear, *Light Alloys*; *Metallurgy of the Light Metals*, 3rd ed., Arnold, London, (1995).

[3] Y. Estrin, M. Yu. Murashkin, R. Z. Valiev, "Ultrafine grained aluminium alloys: processes, structural features and properties", *Fundamentals of Aluminium Metallurgy: Production, Processing and Applications*, Eds. R. Lumley, Woodhead Publishing Limited, Cambridge, pp. 468-503, (2010).

[4] R. Z. Valiev, R. K. Islamgaliev, and I. V. Alexandrov, "Bulk nanostructured materials from severe plastic deformation", *Prog. Mater. Sci.*, Vol. 45, pp. 103-189, (2000).

[5] D. B. Witkin, E. J. Lavernia, "Synthesis and mechanical behavior of nanostructured materials via cryomilling", *Prog. Mater. Sci.*, Vol. 51, pp. 1-60, (2006).

[6] R. Z. Valiev, A. V. Korznikov, and R. R. Mulyukov, "Structure and properties of ultrafine-grained materials produced by severe plastic deformation", *Mater. Sci. Eng.*, Vol. A 168, pp. 141-148, (1993).

[7] Z. Horita, T. Fujinami, and T. G. Langdon, "The potential for scaling ECAP: effect of sample size on grain refinement and mechanical properties", *Mater. Sci. Eng.*, Vol. A 318, pp. 34-41, (2001).

[8] J. Y. Huang, Y. T. Zhu, H. Jiang, and T. C. Lowe, "Microstructures and dislocation configurations in nanostructured Cu processed by repetitive corrugation and straightening", *Acta Mater.*, Vol. 49, pp. 1497-1505, (2001).

[9] Z. Horita, T. Fujinami, M. Nemoto, and T.G. Langdon, "Improvement of mechanical properties for Al alloys using equal-channel angular pressing", *J. Mater. Process. Technol.*, Vol. 117, pp. 288-292, (2001).

[10] A. Shan, I. G. Moon, and J. W. Park, "Estimation of friction during equal channel angular (ECA) pressing of aluminum alloys", *J. Mater. Process. Technol.*, Vol. 122, pp. 255-259, (2002).

[11] S. Ferrasse, V. M. Segal, K. T. Hartwig, and R .E. Goforth, "Microstructure and properties of copper and aluminum alloy 3003 heavily worked by equal channel angular extrusion", *Metall. Mater. Trans.* Vol. A 28, pp. 1047-1057, (1997).

[12] V. M. Segal, "Materials processing by simple shear", *Mater. Sci. Eng.* Vol. A 197, pp. 157-164, (1995).

[13] V. M. Segal, "Equal channel angular extrusion: from macromechanics to structure formation", *Mater. Sci. Eng.*, Vol. A 271, pp. 322-333, (1999).

[14] A. Gholinia, P. B. Prangnell, and M. V. Markushev, "The effect of strain path on the development of deformation structures in severely deformed aluminium alloys processed by ECAE", *Acta Mater.*, Vol. 48, pp. 1115-1130, (2000).

[15] R. Z. Valiev, and T. G. Langdon, "Principles of equal-channel angular pressing as a processing tool for grain refinement", *Prog Mater Sci.*, Vol. 51, pp. 881-981, (2006).

[16] B. Huarte, C. J. Luis, I. Puertas, J. León, and R. Luri, "Optical and mechanical properties of an Al–Mg alloy processed

by ECAE", *J. Mater. Process. Technol.*, Vol. 162, pp. 317-326, (2005).

[17] Y. W. Tham, M. W. Fu, H. H. Hng, M.S. Yong, and K. B. Lim, "Bulk nanostructured processing of aluminum alloy", *J. Mater. Process. Technol.*, Vol. 192, pp. 575-581, (2007).

[18] A. S. M. Agena, "A study of flow characteristics of nanostructured Al-6082 alloy produced by ECAP under upsetting test", *J. Mater. Process. Technol.*, Vol. 209 , pp. 856-863, (2009).

[19] S. Malekjani, P. D. Hodgson, P. Cizek, I. Sabirov, and T. B. Hilditch, "Cyclic deformation response of UFG 2024 Al alloy", *Int. J. Fatigue*, Vol. 33, pp. 700-709 (2011).

[20] Y. Estrin, and A. Vinogradov, "Fatigue behaviour of light alloys with ultrafine grain structure produced by severe plastic deformation: An overview", *Int. J. Fatigue*, Vol. 32, pp. 898-907, (2010).

[21] C. S. Chung, J. K. Kim, H. K. Kim, and W. J. Kim, "Improvement of high-cycle fatigue life in a 6061 Al alloy produced by equal channel angular pressing", *Mater. Sci. Eng.*, Vol. A 337, pp. 39-44, (2002).

[22] P. Huebner, R. Kiessling, H. Biermann, and A. Vinogradov, "Fracture behaviour of ultrafine-grained materials under static and cyclic loading", *Int. J. Mater. Res.*, Vol. 97, pp. 1566-1570, (2006).

[23] P. Huebner, R. Kiessling, H. Biermann, T. Hinkel, W. Jungnickel, R. Kawalla, H. W. Hoeppel, and J. May, "Static and Cyclic Crack Growth Behavior of Ultrafine-Grained Al Produced by Different Severe Plastic Deformation Methods", *Metall. Mater. Trans.*, Vol. A 38, pp. 1926-1933, (2007).

[24] R. Lapovok, C. Loader, F. H. Dalla Torre, and S. L. Semiatin, "Microstructure evolution and fatigue behavior of 2124 aluminum processed by ECAE with back pressure", *Mater. Sci. Eng.*, Vol. A 425, pp. 36-46, (2006).

[25] H. W. Hoeppel, and M. Goeken, "Fatigue behaviour in nanostructured metals", *Nanostructured Metals and Alloys: Processing, Microstructure, Mechanical Properties and Applications*, Eds. S. H. Whang, Elsevier Science, pp. 507-541, (2011).

[26] A. Vinogradov, A. Washikita, K. Kitagawa, and V. I. Kopylov, "Fatigue life of fine-grain Al-Mg-Sc alloys produced by equal-channel angular pressing", *Mater. Sci. Eng.*, Vol. A 349, pp. 318-326, (2003).

[27] A. Vinogradov, and S. Hashimoto, "Multiscale Phenomena in Fatigue of Ultra-Fine Grain Materials-an Overview", *Mater. Trans.*, Vol. 42, pp. 74-84, (2001).

[28] W. J. Kim, J. K. Kim, T. Y. Park, S. I. Hong, D. I. Kim, Y. S. Kim, and J. D. Lee, "Enhancement of strength and superplasticity in a 6061 Al alloy processed by equal-channel-angular-pressing", *Metall. Mater. Trans.* Vol. A 33, pp. 3155-3164, (2002).

[29] H.W. Höppel, M. Kautz, C. Xu, M. Murashkin, T.G. Langdon, R.Z. Valiev, and H. Mughrabi, "An overview: Fatigue behaviour of ultrafine-grained metals and alloys", *Int. J. Fatigue*, Vol. 28, pp. 1001-1010, (2006).

[30] H. W. Höppel, and R. Z. Valiev, "On the possabilities to enhance the fatigue properties of ultrafine-grained metals", *Zeitschrift für Metallkunde*., Vol. 93, pp. 641-648, (2002).

[31] V. Patlan, A. Vinogradov, K. Higashi, and K. Kitagawa, "Overview of fatigue properties of fine grain 5056 Al-Mg alloy processed by equal-channel angular pressing", *Mater. Sci. Eng.*, Vol. A 300, pp. 171-182, (2001).

[32] H. Mughrabi, and R. Wang, "Cyclic stress–strain response and high-cycle fatigue behaviour of copper polycrystals", *Basic mechanisms in fatigue of metals,* Eds. P. Lukas, J. Polak, Elsevier Academia, pp. 1-16, (1988).

[33] H. Mughrabi, H.W. Höppel, and M. Kautz, "Fatigue and microstructure of extrusion with subsequent high-

temperature short-time aging", *Mater. Sci. Eng.,* Vol. 503, pp. 167-171, (2009).ultrafine-grained metals produced by severe plastic deformation", *Scripta Mater*., Vol. 51, pp. 807-812, (2004).

[34] H. Mughrabi, H. W. Höppel, M. Kautz, and R. Z. Valiev, "Annealing treatments to enhance thermal and mechanical stability of ultrafine-grained metals produced by severe plastic deformation", *Zeitschrift für Metallkunde*., Vol. 94, pp. 1079-1083, (2003).

[35] K. Hockaufa, T. Niendorf, S. Wagnera, T. Hallea, and L. W. Meyer, "Cyclic behavior and microstructural stability of ultrafine-grained AA6060 under strain-controlled fatigue", *Procedia Engineering,* Vol. 2, pp. 2199-2208, (2010).

[36] V. D. Sitdikov, P. S. Chizhov, M. Yu. Murashkin, A. A. Goidenko, R. Z. Valiev, "X-ray studies of dynamic aging in an aluminum alloy subjected to severe plastic deformation", *Mater. Charact.*, Vol. 110, pp. 222-227, (2015).

[37] A. Vinogradov, S. Nagasaki, V. Patlan, K. Kitagawa, and N. Kawazoe, *Nanostruct. Mater.*, Vol. 11, pp. 925–934, (1999).

[38] M. Furukawa, Y. Iwahashi, Z. Horita, M. Nemoto, and T. G. Langdon,"The shearing characteristics associated with equal-channel angular pressing", *Mater. Sci. Eng.*, Vol. A 257, pp. 328-332, (1998).

[39] S. S. Manson, and M. H. Hirschberg, "fatigue- an Interdisciplinary approach", Eds. J. J. Burke, V. Weiss, Syracuse University Press, p 231, (1970).

[40] [40] [40]M. Hockauf, L. W. Meyer, B. Zillmann, M. Hietschold, S. Schulze, and L. Krüger, "Simultaneous improvement of strength and ductility of Al-MgSi alloys by combining equal-channel angular extrusion with subsequent high-temperature short-time aging", *Mater. Sci. Eng.,* Vol. 503, pp. 167–171, (2009).

[41] P. Cavaliere, "Mechanical Properties of Nanocrystalline Materials", Ed. M. Aliofkhazraei, *Handbook of Mechanical Nanostructuring*, Wiley–VCH, Weinheim, pp. 3-5, (2015).

[42] *MIL-HDBK-5H*,"Metallic materials and elements for aerospace vehicle structures", *Military handbook,* , Department of defense of the USA, Chapter 3, P. 277, (1998).

[43] K. S. Kumar, H. Van Swygenhoven, and S. Suresh, "Mechanical behavior of nanocrystalline metals and alloys", *Acta. Mater.*, Vol. 51, pp. 5743–5774, (2003).

[44] D. Steiner, and V. Gerold, "The fatigue behaviour of age-hardened Cu-2at.%Co alloy", *Mater. Sci. Eng.*, Vol. 84, pp. 77-88, (1986).

[45] C. Calabrese, and C. Laird, "Cyclic stress–strain response of two-phase alloys part I. Microstructures containing particles penetrable by dislocations", *Mater. Sci. Eng.*, Vol. 13, pp. 141-157, (1974).

[46] C. Calabrese, and C. Laird, "Cyclic stress–strain response of two-phase alloys part II. Particles not penetrated by dislocations", *Mater. Sci. Eng.,* Vol. 13, pp. 159-174, (1974).

[47] S. Horibe, C. Laird, "Orientation and history dependence of cyclic deformation in Al–Cu single crystals containing θ′ precipitates", *Acta. Metall.* Vol. 31, pp. 1567-1579, (1983).

How to cite this paper:

M. Jooybari, J. Shahbazi Karami and M. Sheikhi," Enhancing the low cycle fatigue strength of AA6061 aluminum alloy by using the optimized combination of ECAP and precipitation hardening", *Journal of Computational and Applied Research in Mechanical Engineering*, Vol. 6. No. 2, pp. 115-127

DOI: 10.22061/jcarme.2017.603

URL: http://jcarme.srttu.edu/?_action=showPDF&article=603